IOPscience iopscience.iop.org

Home Search Collections Journals About Contact us My IOPscience

Effect of free carriers on electron mass and infrared absorption in n-type $CdGeAs_2$

This article has been downloaded from IOPscience. Please scroll down to see the full text article.

2006 J. Phys.: Condens. Matter 18 2741

(http://iopscience.iop.org/0953-8984/18/9/011)

View the table of contents for this issue, or go to the journal homepage for more

Download details:
IP Address: 129.252.86.83
The article was downloaded on 28/05/2010 at 09:02

Please note that terms and conditions apply.

INSTITUTE OF PHYSICS PUBLISHING JOURNAL OF PHYSICS: CONDENSED MATTER

J. Phys.: Condens. Matter **18** (2006) 2741–2747 doi:10.1088/0953-8984/18/9/011

Effect of free carriers on electron mass and infrared absorption in n-type $CdGeAs_2$

Chunchuan Xu, Lihua Bai[1] and N C Giles[2]

Physics Department, West Virginia University, Morgantown, WV 26506, USA

E-mail: Nancy.Giles@mail.wvu.edu

Received 6 January 2006
Published 17 February 2006
Online at stacks.iop.org/JPhysCM/18/2741

Abstract

The electrical and optical properties of n-type $CdGeAs_2$ crystals doped with indium have been studied at room temperature using van der Pauw Hall measurements, infrared absorption, and infrared reflectance. Free-electron concentrations (n) in the sample set range from 2.3×10^{17} to 4.3×10^{18} cm^{-3} at 300 K. For the higher levels of free carriers, conduction-band non-parabolicity causes significant increases in electron effective mass m^*. Infrared absorption due to free carriers is consistent with ionized impurity scattering, and absorption coefficients α_f for different samples agree with theoretical predictions when the dependence of m^* on n is included. A relation between α_f and n has been determined for $CdGeAs_2$:In that can be applied to large-sized samples used in nonlinear optical applications. The optical effective mass m^*_{opt} obtained from reflectance data is also in good agreement with predicted m^* values for $CdGeAs_2$.

1. Introduction

Cadmium germanium arsenide ($CdGeAs_2$) is a promising nonlinear optical material for use in infrared frequency conversion devices. It has a high nonlinear optical coefficient and intrinsic transparency in the mid-infrared. The band gap of this chalcopyrite material is about 0.57 eV (2.2 μm) at room temperature [1]. Large, crack-free single crystals have been grown using the horizontal gradient freeze (HGF) technique [2–4], and laser devices that demonstrate second harmonic generation, optical parametric generation, and difference frequency generation have been reported [5–8].

$CdGeAs_2$ crystals grown by the HGF technique are usually p-type due to two native defects (a shallow Ge_{As} acceptor and a deep acceptor) [9]. The tetragonal distortion associated with

[1] Present address: Physics Department, Fisk University, Nashville, TN 37208, USA.
[2] Author to whom any correspondence should be addressed.

© 2006 IOP Publishing Ltd Printed in the UK

the chalcopyrite crystal structure produces a splitting of the top two valence bands (V_1 and V_2) at $\boldsymbol{k} = 0$. This energy splitting, when coupled with a sizable concentration of holes in the uppermost valence band in p-type material, causes an absorption band peaking near 5.5 μm. Specifically, this absorption is an intervalence band transition from V_2 to V_1 [9, 10], and it limits the performance of $CdGeAs_2$ crystals used in nonlinear optical devices. Additional absorption bands lying closer to the band edge have been resolved in p-type material, and their temperature and polarization dependences have been reported [11]. The need to minimize or eliminate the intervalence band absorption at 5.5 μm, however, continues to be the primary focus of recent $CdGeAs_2$ crystal growth efforts. Elimination of the native acceptors during growth is a preferred solution, but an alternative means to reduce the 5.5 μm absorption is to compensate these acceptors by intentional doping with donor impurities.

Doping $CdGeAs_2$ crystals with indium, selenium, and tellurium has resulted in n-type conductivity [12–14]. Indium is expected to incorporate on the Cd site in $CdGeAs_2$ and behave as a singly ionized donor. In a photoluminescence (PL) study of $CdGeAs_2$:In crystals, doping with indium was shown to eliminate the emission band peaking near 0.35 eV that has been attributed to the deep native acceptor [14]. In contrast, doping with Se or Te (on the As site) suppressed the PL emission at 0.55 eV due to the shallow acceptor, but the 0.35 eV emission was still observed. The deeper acceptors remaining in the Se or Te doped samples give rise to absorption in the 3–5 μm region [11] that can affect laser device performance. From the prior PL study of n-type crystals [14], doping with indium (i) suppresses formation of the deep acceptor and (ii) compensates the remaining shallow Ge_{As} acceptors. This, in principle, improves the optical transparency of the $CdGeAs_2$ crystals. Unfortunately, it is commonly observed that doping with indium provides too many free electrons, and free-carrier absorption then limits device performance.

In the present paper, we describe a study of the electrical and optical properties of $CdGeAs_2$ crystals heavily doped with indium donors. An increase in electron effective mass m^*, due to the conduction-band non-parabolicity, is used to explain the magnitudes of free-carrier absorption in this sample set. For two samples with $n > 2 \times 10^{18}$ cm^{-3}, we use infrared reflectance data to determine optical effective masses m^*_{opt}, which are also in good agreement with the predicted increases in m^*.

2. Experiment setup

The present study includes ten n-type indium-doped $CdGeAs_2$ crystals grown by the HGF technique. These samples were cut from three different boules. Two boules were grown at Stanford University (Palo Alto, CA) and one boule was grown at BAE Systems (Nashua, NH). The growth and PL properties of these samples have been previously described [14]. For the optical measurements, oriented samples approximately 4×4 mm^2 and between 1 and 2 mm in thickness were cut with the broad faces normal to the [001] direction (i.e., the samples are c plates). The optical faces were mechanically polished using diamond paste down to 0.1 μm. For reflectance data, one of the polished surfaces for each sample was additionally chemipolished using a 2% bromine in ethylene glycol mixture, followed by a free etch in a 2% bromine in methanol solution.

Absorption and reflectance data were taken with a Thermo Nicolet Nexus 870 Fourier-transform infrared spectrometer (FTIR) purged with N_2 gas. A DTGS detector and a KBr beamsplitter were used. The sample thickness and reflective losses at the two air/sample surfaces were accounted for when converting the measured absorption data (in optical density or O.D.) to absorption coefficient (in cm^{-1}). Reflectance experiments were performed over the range 3–27 μm using a specular reflectance accessory and an aluminium mirror for reference.

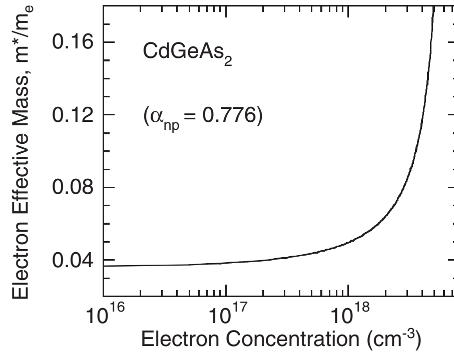

Figure 1. Electron effective mass versus electron concentration in $CdGeAs_2$. The conduction band non-parabolicity is included, according to equation (3).

Data showing the reflectance minima due to plasma oscillations were obtained from two n-type samples with high electron concentrations.

Hall-effect data were taken on a commercial system from MMR Technologies, using a van der Pauw geometry and indium solder contacts. The carrier concentrations and carrier mobilities reported here were determined using a Hall factor r of 1 (i.e., $n_H = n$ and $\mu_H = \mu$).

3. Results and discussion

At sufficiently high doping densities, an increase in the carrier effective mass (m^*) is observed in many semiconductors [15–17]. The concentration dependence of m^* is given by

$$\frac{1}{m^*} = \frac{1}{m_0^*}\left(1 - \frac{2\phi}{E_g}\right) \tag{1}$$

where m_0^* is the effective mass at $\boldsymbol{k} = 0$ assuming a parabolic band, E_g is the band gap at $\boldsymbol{k} = 0$, and ϕ is a function of the carrier density n and the dimensionless non-parabolicity coefficient α_{np}. In particular,

$$\phi = \alpha_{np}\left(3\pi^2 n\right)^{2/3}\left(\frac{\hbar^2}{2m_0^*}\right). \tag{2}$$

An expression for α_{np}, appropriate for non-zero crystal-field splittings, is given by equation (16) in [14]. For n-type $CdGeAs_2$, using $E_g = 0.57$ eV, $m_0^* = 0.036m_e$ (where m_e is the free-electron mass) [18], and $\alpha_{np} = 0.776$, equation (1) can be rewritten as

$$\frac{1}{m^*} = \frac{1}{0.036m_e}\left(1 - 2.75 \times 10^{-13} n^{2/3}\right). \tag{3}$$

Figure 1 is a graph of equation (3) showing the dependence of m^* on n. Free-electron concentrations in $CdGeAs_2$ at levels exceeding mid-10^{17} cm^{-3} begin to cause significant increases in m^*, and corresponding changes in relaxation times and scattering rates are expected to affect optical absorption behaviours. Table 1 provides the experimentally measured electron concentrations and electron mobilities and the calculated effective masses for the ten n-type $CdGeAs_2$ samples included in the present study.

Next, we turn to optical data from our n-type samples and test the validity of a concentration-dependent m^*. Representative absorption spectra are shown in figure 2 for three of the In-doped samples. In these n-type samples, the discrete intervalence band absorption

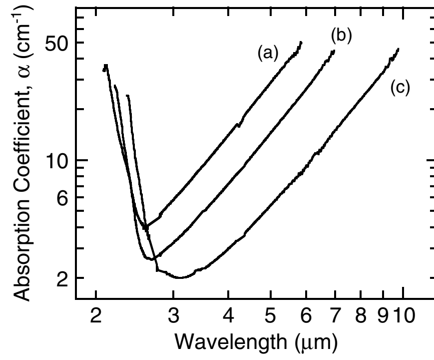

Figure 2. Absorption coefficient versus wavelength for three n-type $CdGeAs_2$ samples. The labels (a)–(c) correspond to the sample identities used in table 1.

Table 1. Summary of Hall data, predicted electron effective masses (using equation (3)), and infrared absorption exponents (p) for $CdGeAs_2$:In samples. Absorption power-law behaviour ($\alpha \sim \lambda^p$) was used to determine p. Optical effective masses (m^*_{opt}) were determined for two samples using the reflectance minimum.

Sample	Hall data at 300 K n (in cm^{-3})	Hall data at 300 K μ (in $cm^2\ V^{-1}\ s^{-1}$)	Predicted mass m^*/m_e	p from $\alpha \sim \lambda^p$	Measured optical mass m_{opt^*}/m_e
a[a]	4.3×10^{18}	1030	0.138	3.4	0.13
b[a]	2.7×10^{18}	970	0.079	3.5	0.12
c[a]	4.6×10^{17}	200	0.041	3.4	—
d[b]	2.9×10^{18}	990	0.084	3.3	—
e[b]	1.9×10^{18}	1390	0.062	3.5	—
f[b]	1.8×10^{18}	1490	0.061	3.5	—
g[b]	1.6×10^{18}	1360	0.058	3.4	—
h[b]	1.5×10^{18}	1420	0.057	3.5	—
i[b]	3.3×10^{17}	2040	0.041	3.2	—
j[b]	2.3×10^{17}	2770	0.040	3.3	—

[a] Grown at BAE Systems.
[b] Grown at Stanford University.

at 5.5 μm is completely eliminated, and the increase in absorption coefficient α at longer wavelengths is due to free carriers (i.e., electrons). The absorption coefficient follows the expression $\alpha_f \sim \lambda^p$ [19], where the exponent p can vary from 1.5 to 3.5 depending on the dominant scattering mechanism in the material. See table 1 for the p values determined for the $CdGeAs_2$ samples used in this study. In general, acoustic-phonon scattering will be described by $p \approx 1.5$ [20], scattering by optical phonons gives $p \approx 2.5$ [21], and scattering by ionized impurities is described by $p \approx 3$ or 3.5 [20]. All three kinds of scattering may occur, but the dominant mechanism depends on impurity concentration and sample quality. Ionized-impurity scattering is consistent with the p values determined for these $CdGeAs_2$:In samples.

Since the power-law dependence of α_f on λ suggests that ionized-impurity scattering is dominant, the absorption coefficient should have the following functional form [20]:

$$\alpha_f = \frac{n\mathrm{N}_i}{(m^*)^{1.5}}\lambda^{3.5}(\times\mathrm{Constant}) \qquad (4)$$

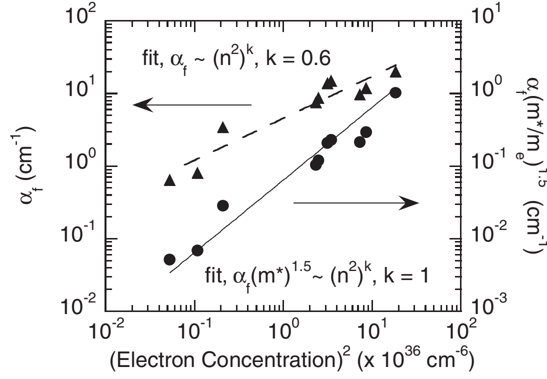

Figure 3. Correlation between optical and electrical data for n-type $CdGeAs_2$:In samples. Using filled triangles, the absorption coefficient (α_f) due to free carriers is plotted versus n^2, and shows a sublinear power dependence. Using filled circles, the linear dependence of the product α_f* (effective mass)$^{1.5}$ on n^2 is shown.

where N_i is the concentration of ionized centres, and n and m^* have their previous meanings. For intrinsic $CdGeAs_2$, the 300 K electron concentration is approximately 2.6×10^{13} cm^{-3}. Hole concentrations of 10^{15}–10^{16} cm^{-3} are typically observed in high-quality crystals due to native acceptors. If a sufficient indium doping level is used to compensate these acceptors and produce $n > 10^{17}$ cm^{-3}, we can assume $N_i \approx n$. Thus, the absorption at a particular spectral position should vary as $\alpha_f \sim n^2(m^*)^{-1.5}$. Experimental values of absorption coefficients at 5 μm are then used to evaluate whether a concentration-dependent m^* is needed. This particular wavelength was chosen since α_f values could be determined for all ten samples (i.e., at longer wavelengths, the absorbance for the most heavily doped samples was out of the spectrometer absorbance range). The results are shown in figure 3 as either α_f versus n^2 (see left vertical axis) or $\alpha_f(m^*)^{1.5}$ versus n^2 (see right vertical axis). The m^* values for the latter comparison were determined using equation (3). Note that each vertical axis spans four decades, and a sublinear power-law behaviour in the α_f versus n^2 plot is clearly indicated, showing that the absorption at a particular spectral position in these samples cannot be explained using a constant electron effective mass. The dashed line is a best fit to a power-law relation of the form $\alpha_f \sim (n^2)^k$ and gives $k = 0.6$. The solid line is a best fit showing a linear relation between α_f and $n^2(m^*)^{-1.5}$. Here, even the highest doped samples follow the trend, and the large predicted increases in m^* are consistent with the measured α_f intensities.

A correlation between α_f and n, based on equation (4), yields the following expression for n-type $CdGeAs_2$:In.

$$\alpha_f = (6.51 \times 10^{-38})n^2(1 - 2.75 \times 10^{-13}n^{2/3})\lambda^p. \quad (5)$$

Here, α_f, n, and λ have units of cm^{-1}, cm^{-3}, and μm, respectively, and $p \approx 3.5$. Many of today's $CdGeAs_2$ crystals have large dimensions (many mm in thickness) and are intended for use in frequency conversion laser devices. Thus, equation (5) allows a determination of 'over-doping' in samples with long optical path lengths, and having dimensions that are inappropriate for Hall measurements.

The free-carrier effects on sample reflectivity also depend on carrier mass. The reflectivity will reach a minimum near the plasma resonance frequency of the sample. A previous study using plasma reflection [22] showed an increase in m^*_{opt} in n-type $CdGeAs_2$ from $0.034m_e$ to $0.074m_e$ for samples in the high-10^{17} to mid-10^{18} cm^{-3} range. These mass values are low

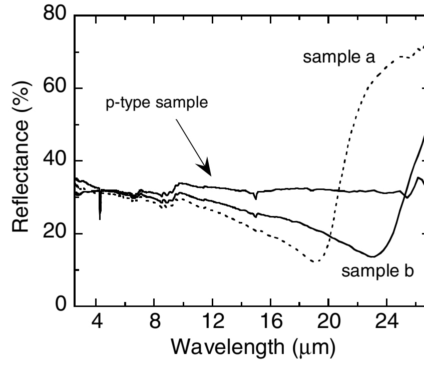

Figure 4. Reflectance spectra at room temperature for (a) n-type $CdGeAs_2$:In, sample a; (b) n-type $CdGeAs_2$:In, sample b; and (c) p-type $CdGeAs_2$ ($p_{300\ K} = 4 \times 10^{16}$ cm^{-3}).

compared to our expectations based on equation (3). The plasma resonance wavelength λ_p can be described by the following expression (in SI units):

$$\lambda_p = \frac{2\pi c (m^*_{opt}\varepsilon_{opt}\varepsilon_0)^{\frac{1}{2}}}{(ne^2)^{\frac{1}{2}}} \quad (6)$$

where n is the electron concentration, m^*_{opt} is the effective mass of the carriers, ε_{opt} is the optical dielectric constant, and ε_0 is the vacuum permittivity. In the ideal case, the reflectance R will decrease to zero at a wavelength corresponding to

$$\lambda = \sqrt{\frac{\varepsilon_{opt} - 1}{\varepsilon_{opt}}}\lambda_p. \quad (7)$$

Reflectance spectra from samples a and b are shown in figure 4, and a spectrum from a p-type sample is included for reference. Since these n-type samples have fairly high absorption in the infrared, contributions due to multiple reflections should be small. Reflection minima occur at about 19.3 and 23.1 μm for these two samples. For lower-doped samples, the reflectance did not vary much within this spectral range. The plasma resonance wavelengths calculated using equation (7) and $\varepsilon_{opt} = 12$ are 20.2 and 24.0 μm for samples a and b, respectively. The m^*_{opt} values determined using equation (6) and λ_p are $0.13m_e$ and $0.12m_e$. These values are higher than those reported in [22]. The m^*_{opt} value for sample a agrees very well with the predicted concentration-dependent m^*, while the m^*_{opt} value obtained for sample b is about 50% too high. Some error is expected in our comparison of m^* and m^*_{opt}, since we assume a Hall r factor of 1; however, this error should be small and will affect results for both samples. The discrepancy between m^* and m^*_{opt} for sample b could be taken as evidence of a non-uniform dopant distribution in this particular sample resulting in a higher free-carrier concentration near the surface. In a non-uniform sample, the reflectance data, which is affected by the material properties near the surface, may not agree with an overall averaged result like that obtained from Hall data. Infrared absorption data and Hall data would still show good agreement since they are both 'averaged' over the same sample thickness.

4. Conclusion

The concentration dependence of the electron effective mass m^* has been evaluated and shown to affect optical absorption spectra in n-type $CdGeAs_2$. The free-carrier absorption in n-type $CdGeAs_2$ crystals follows a $n^2(m^*)^{-1.5}$ dependence, consistent with ionized impurity

scattering. The magnitudes of the m^* increases were further supported using infrared reflectance data for two heavily doped n-type samples.

Acknowledgments

The authors wish to thank R S Feigelson (Stanford University) and P G Schunemann (BAE Systems) for providing the n-type $CdGeAs_2$ samples. The work was supported by the Air Force Office of Scientific Research under grant number F49620-01-1-0428.

References

[1] Shileika A 1973 *Surf. Sci.* **37** 730
[2] Schunemann P G and Pollak T M 1997 *J. Cryst. Growth* **174** 272
[3] Schunemann P G and Pollak T M 1998 *Mater. Res. Soc. Bull.* **23** 23
[4] Schunemann P G, Setzler S D, Pollak T M, Ptak A J and Myers T H 2001 *J. Cryst. Growth* **225** 440
[5] Schunemann P G and Pollak T M 1998 *Mater. Res. Soc. Bull.* **23** 1096
[6] Zakel A, Blackshire J L, Schunemann P G, Setzler S D, Goldstein J and Guha S 2002 *Appl. Opt.* **41** 2299
[7] Vodopyanov K L and Schunemann P G 1998 *Opt.Lett.* **23** 1096
[8] Vodopyanov K L, Knippels G M H, Van der Meer A F G, Maffetone J P and Zwieback I 2002 *Opt. Commun.* **202** 205
[9] Bai L, Poston J A Jr, Schunemann P G, Nagashio K, Feigelson R S and Giles N C 2004 *J. Phys.: Condens. Matter* **16** 1279
[10] Mamedov B Kh and Osmanov É O 1972 *Sov. Phys.—Semicond.* **5** 1120
[11] Bai L, Giles N C and Schunemann P G 2005 *J. Appl. Phys.* **97** 023105
[12] Borshchevskii A S, Goryunova N A, Osmanov E O, Polushina I K, Royenkov N D and Smirnova A D 1968/1969 *Mater. Sci. Eng.* **3** 118
[13] Bairamov B H, Rud V Yu and Rud Yu V 1998 *Mater. Res. Soc. Bull.* **23** 41
[14] Bai L, Xu C, Nagashio K, Chunhui Y, Feigelson R S, Schunemann P G and Giles N C 2005 *J. Phys.: Condens. Matter* **17** 5687
[15] Raymond A, Robert J L and Bernard C 1979 *J. Phys. C: Solid State Phys.* **12** 2289
[16] Bugajski M and Lewandowski W 1985 *J. Appl. Phys.* **57** 521
[17] Yoon I T, Ji T S, Oh S J, Choi J C and Park H L 1997 *J. Appl. Phys.* **82** 4024
[18] Kildal H 1974 *Phys. Rev.* B **10** 5082
[19] Pankove J I 1971 *Optical Processes in Semiconductors* (New York: Dover)
[20] Fan H Y, Spitzer W G and Collins R J 1956 *Phys. Rev.* **101** 566
[21] Visvanathan S 1960 *Phys. Rev.* **120** 376
[22] Zlatkin L B, Markov Yu F and Polushina I K 1969 *Sov. Phys.—Semicond.* **3** 1336